We are IntechOpen,
the world's leading publisher of
Open Access books
Built by scientists, for scientists

4,800

Open access books available

122,000

International authors and editors

135M

Downloads

Our authors are among the

154

Countries delivered to

TOP 1%

most cited scientists

12.2%

Contributors from top 500 universities

CLARIVATE ANALYTICS
BOOK CITATION INDEX
INDEXED

WEB OF SCIENCE™

Selection of our books indexed in the Book Citation Index
in Web of Science™ Core Collection (BKCI)

Interested in publishing with us?
Contact book.department@intechopen.com

Numbers displayed above are based on latest data collected.
For more information visit www.intechopen.com

Graphene Transistors and RF Applications

Jeong-Sun Moon[1], Kurt Gaskill[2] and Paul Campbell[2]
[1]HRL Laboratories,
[2]United States Naval Research Laboratory,
U.S.A

1. Introduction

Graphene is an atomically thin but stable layer form of hexagonal carbon and has attracted a lot of attention in the research community over the last few years because of its unique electronic properties [Geim & Novoselov, 2007; Guisinger and Arnold, 2010]. Graphene exhibits the highest carrier mobility: >100,000 cm^2 V^{-1} s^{-1} at room temperature [Morozov et al., 2008]. This is not only ~100 times greater than that of Si, but about 10 times greater than state-of-the-art semiconductors lattice-matched to InP, currently regarded the best high-speed materials. The saturation velocity (v_{sat}) of graphene has not been determined clearly yet, but it is estimated to be ~5 times greater than that for Si MOSFETs [Akturk and Goldsman, 2008]. With expected large on-state current density and transconductance per gate capacitance compared to Si, graphene has the potential to offer excellent switching characteristics (capacitance/on-state current) and short-circuit current gain cut-off frequency. Although it is too early to predict, graphene FETs could potentially be processed in a manner compatible with Si CMOS with desirable integration density for system-on-chip applications. While there are numerous challenges (including proper bandgap engineering) to be overcome for graphene to become a mature technology, this material offers unique device and circuit applications including ambipolar RF electronics [Moon et al., 2009].

2. Epitaxial graphene synthesis

Several epitaxial graphene synthesis approaches have been reported on the wafer-scale, including a Si sublimation method out of SiC substrates [Berger et al., 2004 & 2006], metal catalyst-based CVD growth [Sutter, 2008] and direct carbon deposition in MBE.

3. Epitaxial graphene transistors

Epitaxial graphene FETs on the wafer-scale are in early stages of development, although several key device parameters have been demonstrated. For example, epitaxial graphene RF FETs have been demonstrated in a top-gated layout with the highest ever on-state current density of 3 A/mm [Moon et al., 2009 #2]. In addition, the extrinsic speed performance (f_t/f_{max} of 5 GHz/14 GHz) is reported with a 2 μm gate length [Moon et al., 2009 #2]. On the other hand, the current-voltage characteristics are quasi-linear with weak saturation behaviors, yielding low transconductance (gm) per capacitance (i.e., <140 mS/mm at 3.4 fF/μm^2) and poor voltage gain (gm/G_{ds}). Also, the I_{on}/I_{off} ratio was ~4 with field-effect mobility below 200

cm^2/Vs. While graphene field-effect mobility as high as 5400 cm^2/Vs for electron has been demonstrated [Wu et al., 2008], it was achieved using six to seven layers of epitaxial graphene on C-face SiC substrates, resulting in an I_{on}/I_{off} ratio of <2. In the case of graphene FETs fabricated on the Si-face of SiC substrates, field-effect mobility has been limited to below 1200 cm^2/Vs, but with an improved I_{on}/I_{off} ratio of ~10 [Kedzierski et al., 2008].

(a)   (b)   (c)
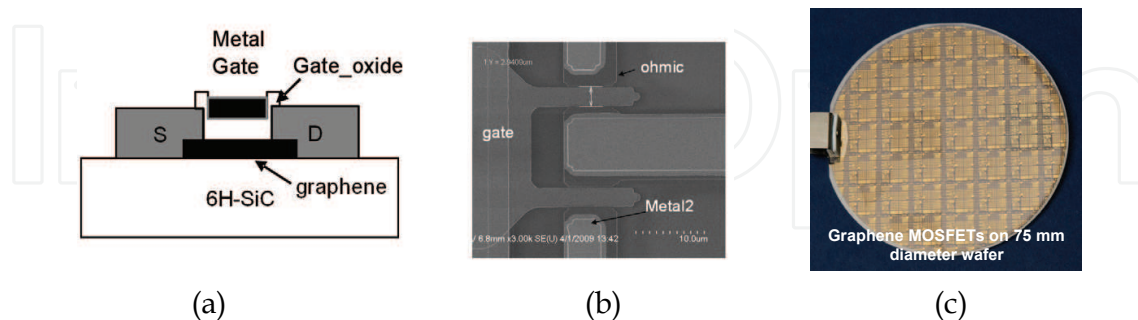
Fig. 1. (a) A schematic of the top-gated graphene FET. (b) A SEM photograph of 2f x 4 μm graphene FET. (c) A photograph of 75 mm graphene wafer.

In this section, we present top-gated graphene n-FETs and p-FETs from epitaxial graphene layers, where *excellent I-V saturation behaviors were observed in epitaxial graphene FETs* with a record peak extrinsic transconductance of 600 mS/mm [Moon et al., 2010]. Also, the effective mobility and field-effect mobility versus E_{eff} were characterized and compared with Hall mobility. The epitaxial graphene layers were grown on Si-face 6H-SiC substrates on 50-mm wafers via Si sublimation [Gaskill et al., 2009]. The sheet electron carrier density of the epitaxial graphene layer was typically 8.8 x 10^{12} cm^{-2} at room temperature and had electron mobility of ~1192 cm^2/Vs, characterized by non-contact Hall Lehighton 1600. The number of epitaxial graphene layers (nGL) was found to be one layer on the SiC terraces and two layers on the step edges over the entire 50-mm wafer as characterized by Raman analysis and transmission electron microscopy analysis.

Graphene FETs were fabricated using Ti/Pt/Au source and drain metal deposition and lift-off process. The non-alloyed ohmic metal yielded the contact resistivity of 10^{-6} – 10^{-7} Ω·cm^2 [Moon et al., 2009 #2]. The metal gates were processed via the Ti/Pt/Au metal deposition and lift-off process on top of a 35-nm-thick SiO_2 gate dielectric layer deposited by electron beam evaporation. The gate leakage current was in the range of ~nA/$μm^2$ or less, which is negligible in the device characterization presented here.

Figure 1 (a)-(c) shows the graphene FET processed in a layout, where the gate metal is aligned with respect to the ohmic metals in an under lap layout with a gate-to-source/drain separation of <100 nm to minimize the access resistance over a source-drain spacing (L_{sd}) of 3 μm. The source access resistance was <0.2 Ω·mm via the standard end-point measurements on transfer length method (TLM) structures. A graphene channel width of 4 μm was defined by O_2 plasma etching.

Figure 2 (a)-(b) shows measured room temperature, common-source, current-voltage characteristics of a two-gatefinger and 4-μm-wide n-channel graphene FET (denoted as 2f x 4 μm), in which excellent drain current saturation was observed. The source-to-drain voltage (Vds) increased to 3 V, where the gate-to-source (Vgs) voltage was stepped from 3 V (top-curve) in steps of -0.5 V. At Vds = 1 V, on-state current at Vgs = 3 V was 0.59 A/mm. The off-state current was 0.047 A/mm at Vgs = -1 V, yielding I_{on}/I_{off} ratio of 12.5. At Vds = 0.5 V, the I_{on}/I_{off} ratio increased to 19 with the on-state current of 0.31 A/mm. At Vds = 3 V, the on-state current at Vgs = 3 V was measured as high as 1.65 A/mm. The on-resistance was 1.6 Ω·mm.
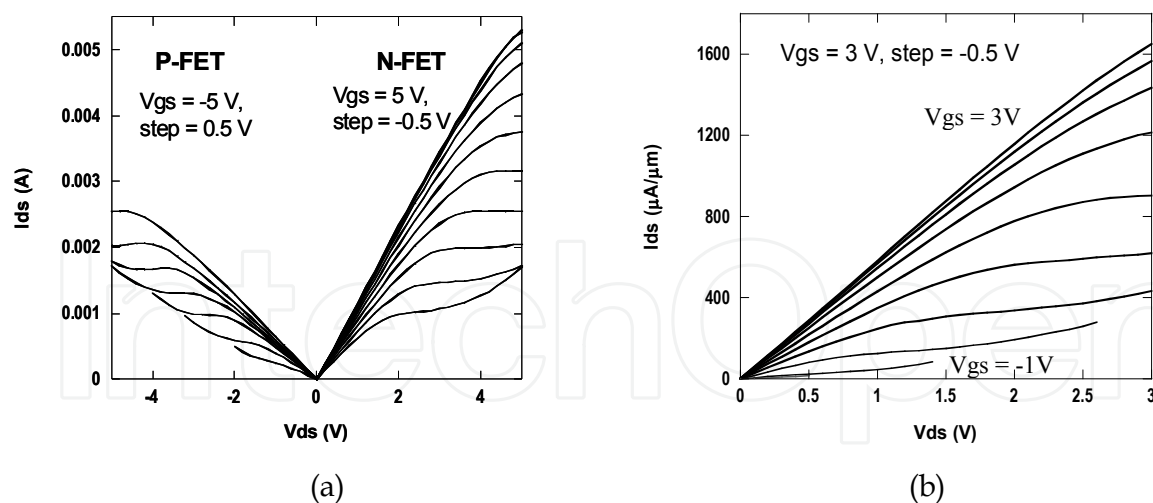
Fig. 2. (a) Measured common-source current-voltage characteristics of 1f x 4 μm graphene FET. (b) Both p-channel and n-channel graphene MOSFET operations.

Figure 3 shows measured transconductance (gm) of a 2f x 4 μm graphene FET at different Vds, stepping from 1.05 to 3.05 V with a step of 0.5 V. The inset shows measured transfer curves. At Vds = 3.05 V, the Ids reached up to 1.1 A/mm at Vgs = 3 V. The ambipolar behavior was observed clearly at Vds >2 V, while the ambipolar behavior is not well-developed with a relatively flat region observed at low Vds such as Vds = 1.05 V. The peak extrinsic gm of 600 mS/mm was measured at Vds = 3.05 V, which is the highest ever, amongst epitaxial graphene FETs. The observed negative transconductance is due to a conversion of n-channel to p-channel. The effective mobility, μ_{eff}, was extracted using a formula: $\mu_{eff} = (L/W) \cdot Ids/[C_{ox} \cdot (Vgs-V_T) \cdot Vds]$. The C_{ox} is gate_oxide capacitance, $\varepsilon_0 \cdot \varepsilon_{ox}/t_{ox}$, where ε_0 and ε_{ox} are permittivity of the free space and gate_oxide layer, respectively. Gate_oxide capacitance is measured using a metal-gate_oxide-metal (MOM) capacitor array with OPEN and SHORT calibration standards. The geometric scaling of the MOM capacitors is verified to eliminate fringe capacitances. The geometric oxide capacitances were measured at 1 fF/μm² or 1.7 fF/μm² from the two different wafers. The dielectric constant of the deposited SiO_2 films was determined to be 3.9, which is close to that of SiO_2. The field-effect mobility, μ_{FE}, defined by $\mu_{FE} = (L/W) \cdot gm/(C_{ox} \cdot Vds)$, was obtained from the transconductance (gm) at Vds = 50 mV. So, there is no ambiguity in μ_{FE} associated with the V_T unlike the case of μ_{eff}. The effective electric field is estimated using $E_{eff} = Q_{Gr}/(\varepsilon_0 \cdot \varepsilon_{ox})$, where Q_{Gr} is the total charge in the graphene channel.

Figure 4 shows extracted μ_{eff} and μ_{FE} of graphene n-FETs versus the effective electric field, E_{eff}. In comparison, the universal and field-effect mobility of Si n-MOSFETs [Takagi et al., 1994] and strained Si n-MOSFETs on SiGe-on-oxide [Cheng et al., 2001] are shown. While both the μ_{eff} and μ_{FE} of the graphene n-FETs depend on E_{eff}, both values were higher than 1000 cm²/Vs over a wide range of the effective electric field up to 1.6 MV/cm. The peak field-effect mobility values ranged from 3200 cm²/Vs to 6000 cm²/Vs. A record field-effect mobility of 6000 cm²/Vs was obtained at an effective electric field of 0.27 MV/cm. The measured field-effect mobility of graphene n-FETs was at least seven times higher than that of ITRS Si n-MOSFETs and ~80 times higher than ultra-thin-body SOI n-MOSFETs. The peak field-effect mobility of graphene p-FETs was also determined to be 3200 cm²/Vs at an effective electric field of 0.2 MV/cm.
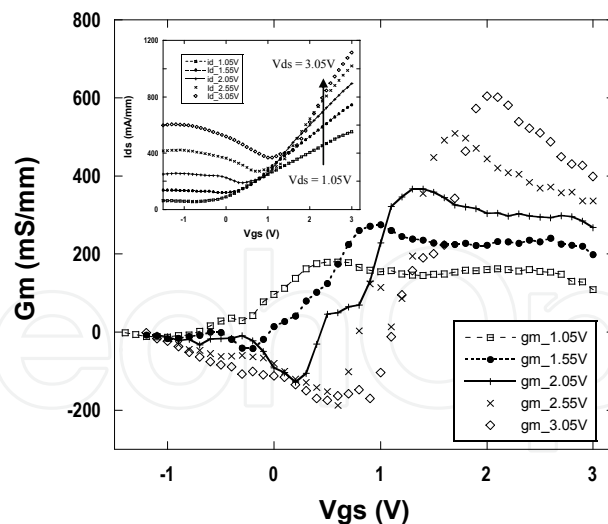
Fig. 3. Measured small-signal transconductance of 1f x 4 μm n-channel graphene FET at different Vds , from 1.05 V to 3.05 V in steps of 0.5 V. Peak extrinsic transconductance is as high as 600 mS/mm at Vds = 3.05 V. The inset shows measured transfer curves from 1.05 V to 3.05 V in steps of 0.5 V.
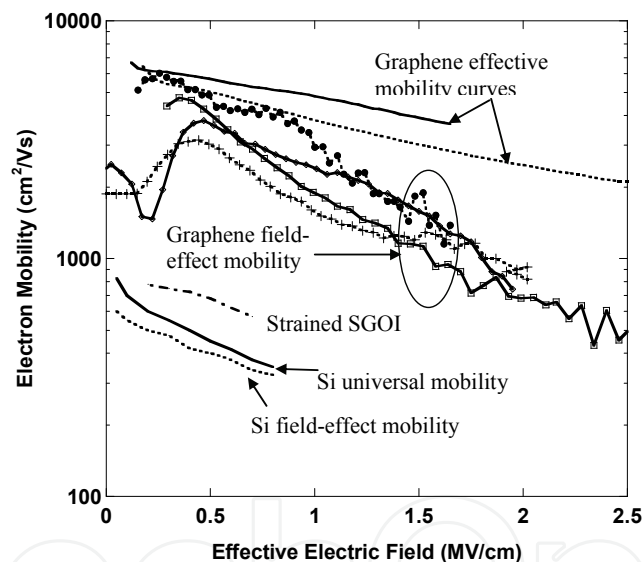

Fig. 4. Measured effective carrier mobility and field-effect mobility of graphene n-FETs compared with those of Si n-MOSFET and strained Si on SGOI MOSFET.

4. Wafer-scale graphene-on-Si transistors

Graphene synthesis directly on silicon substrates is highly attractive because graphene wafers can be scaled-up significantly larger than commercially available (4,6)H-SiC substrates; this technique is being evaluated either via a direct carbon deposition [Hackley et al., 2009] or via a growth of template layer such as 3C-SiC [Suemitsu et al., 2009]. Utilizing a 3C-SiC(111) template grown on Si(110), epitaxial graphene-on-Si FETs are reported with Ion of >0.03 μA/μm at V_{ds} = 1V in a top-gated layout [Kang et al., 2009]. The very low Ion was attributed to a hight sheet resistance of 129 kΩ/sq. Ambipolar current-voltage characteristics, unique to the graphene, were not clearly demonstrated.

In this section, we present top-gated graphene-on-Si FETs utilizing 3C- SiC(111) templates grown on 75 mm Si(111) substrates. The ambipolar characteristics were observed clearly for the first time, with Dirac points close to zero gate voltage. The Ion of 225 μA/μm was demonstrated, which is the highest for epitaxial graphene-on-Si FETs.

Figure 5 shows a schematic of top-gated and self-aligned, graphene-on-Si FETs with a SEM photograph of a 2 gatefinger graphene FET. These graphene-on-Si FETs were processed in a layout with a source-drain spacing (L_{sd}) of 1 or 3 μm; the gate metal is aligned with respect to the pre-defined ohmic metals in an under lap layout with a gate-to-source/drain separation of <100 nm. Graphene channel widths varied from 6 μm, 12 μm, and 25 μm, which were defined by O_2 plasma etching. Ohmic metals were fabricated with Ti/Pt/Au source and drain metal deposition and lift-off process. The non-alloyed ohmic metal yielded a contact resistance of 2.5 Ω·mm and a contact resistivity of ~10^{-5} Ω·cm² using the transmission line method (TLM). The contact resistivity was higher than that of ~10^{-7} Ω·cm² from graphene-on-SiC FETs [6]. The metal gates were processed with Ti/Pt/Au metal deposition and lift-off process on top of a 35-nm-thick SiO_2 gate dielectric layer deposited by electron beam evaporation. Figure 5(c) shows measured transfer curves of 25-μm-wide graphene-on-Si FETs with L_{sd} = 3 μm at a fixed V_{ds} = 2 V. The ambipolar behaviors were observed clearly with Dirac points closed to zero gate voltage. An I_{on} of 80-100 μA/μm was obtained at V_{gs} = 3 V.
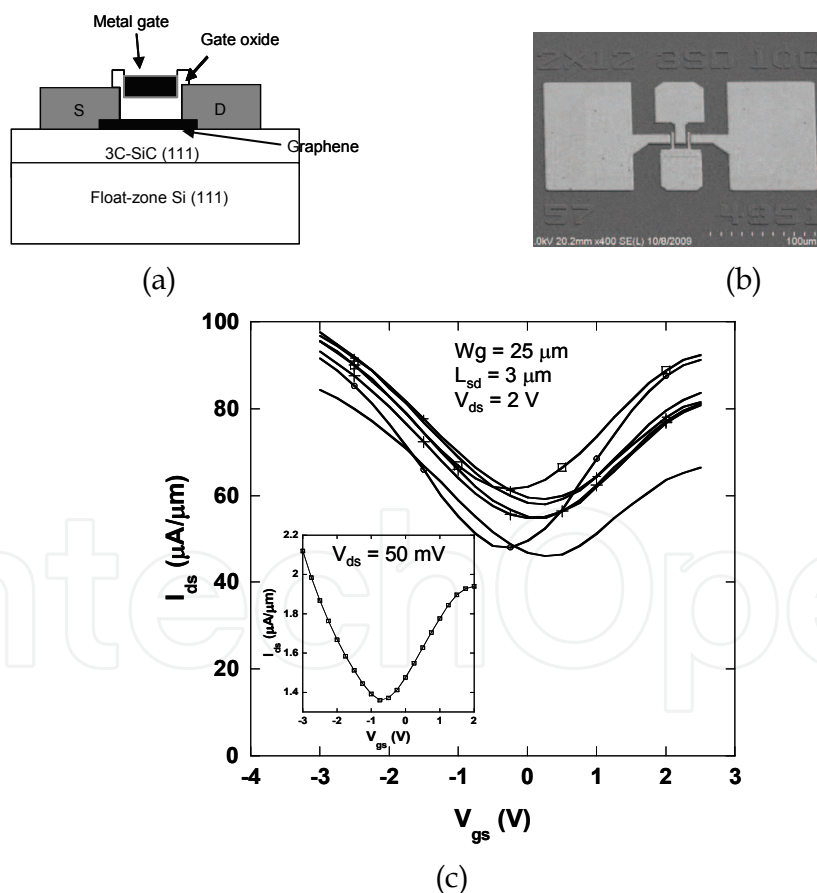

(a)   (b)

(c)

Fig. 5. (a) A schematic of the top-gated graphene FET. (b) A SEM photograph of two-gatefinger and 12-μm-wide graphene FET (denoted as 2f x 12 μm). (c) Measured transfer curve of 1f x 25 μm epitaxial graphene-on-Si FETs at V_{ds} = 2 V with ambipolar behaviors. The L_{sd} was 3 μm. The inset shows measured transfer curve at V_{ds} = 50 mV.

5. RF Applications

Figure 6(a) shows measured $|H_{21}|$ and unilateral gain (U) of the 2 x 12 µm graphene FETs at Vds = 5 V with source-drain spacing (Lds) of 3 µm. The extrinsic f_T and f_{max} are 2.7 GHz and 3.4 GHz, respectively. Figure 6(b) shows measured plots of magnitude of H_{21} ($|H_{21}|$) and unilateral gain (U) of the 2 x 12 µm graphene FETs with source-drain spacing (Lds) of 1 µm. The S-parameters were measured at Vds = 5 V and Vgs = -2.5 V. An extrinsic cut-off frequency (f_T) of 4.1 GHz was extracted, yielding an extrinsic $f_T \cdot L_g$ of 8.2 GHz·µm. The extrinsic gm was 195 mS/mm. A maximum oscillation frequency (f_{max}) of 11.5 GHz was extracted from the unilateral gain (U) with a slope of -20 dB/decade. Figure 7 shows a plot of extrinsic f_T and f_{max} measured from both of the graphene FETs. For graphene FET #1, the extrinsic gm improved to 148 mS/mm at Vds = 9 V, yielding the extrinsic f_T and f_{max} of 4.4 GHz and 6 GHz, respectively. For graphene FET #2, the f_T and f_{max} were 4.2 GHz and 14 GHz, respectively, at Vds = 7 V. With a source access resistance of 1.9 Ω·mm, the intrinsic gm becomes 205 mS/mm. This yields an intrinsic f_T of 5 GHz with an intrinsic $f_T \cdot L_g$ of 10 GHz·µm, which is slightly better than 8.9 GHz·µm from the bulk Si NMOS. At present, the RF performance of graphene FETs is not close to what had been predicted by the intrinisc saturation velocity of the graphene channel, 4-5E7 cm/sec. The $f_T \cdot L_g$ product of graphene FETs is expected to improve as the quality of the epitaxial graphene layer and transistor fabrication processing improve with reduced parasitic charging delay, such as (Rs +Rd)*Cgd [Moon e tal., 2008]. The unique ambipolar nature of graphene FETs can benefit various RF circuit applications, such as frequency multipliers, mixers and high-speed radiometers. The future success of the RF circuit applications depends on vertical and lateral scaling of graphene MOSFETs to minimize parasitics and improve gate modulation efficiency in the channel.
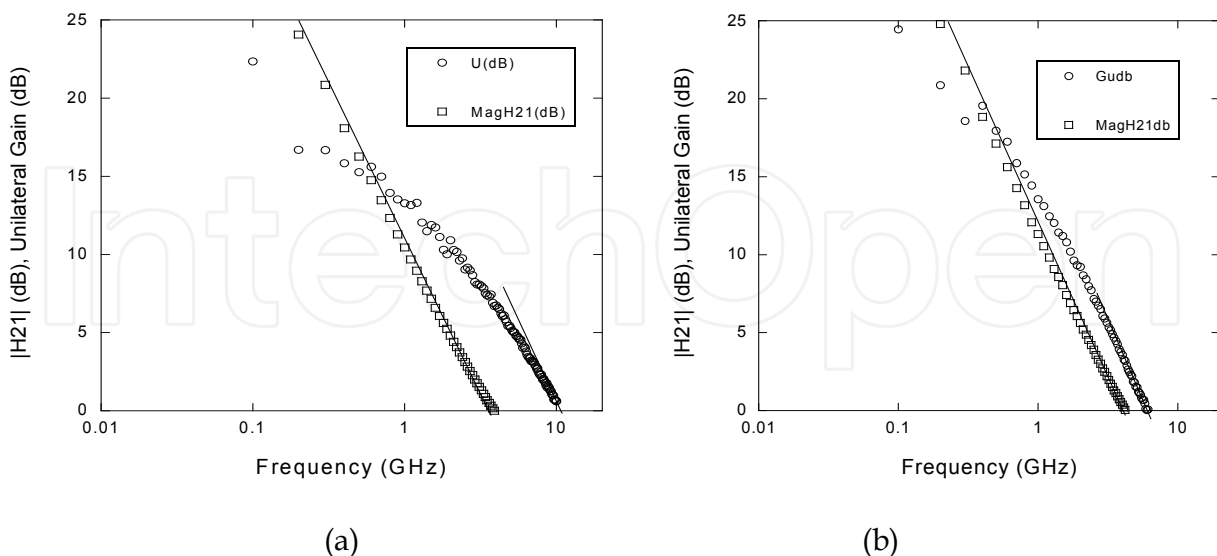

Fig. 6. Measured $|H_{21}|$ and unilateral gain (U) are shown as a function of frequencies at Vds = 5 V and Vgs = -2.5 V of 2 x 12 µm graphene MOSFETs with (a) Lds = 3 µm and (b) Lds = 1 µm.
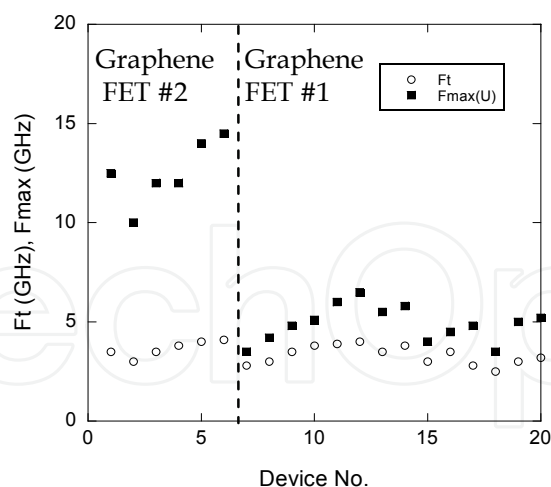
Fig. 7. A plot of measured extrinsic f_T and f_{max} of the graphene FETs is shown. The gate length is 2 μm. The highest ft and fmax are 4.1 GHz and 14 GHz, respectively.

6. References

A. K. Geim and K. S. Novoselov, "The rise of graphene", Nature Materials, vol. 6, pp 183-191, 2007.

N.P. Guisinger and M.S. Arnold, "Beyond Silicon: Carbon-based Nanotechnology", MRS Bulletin, vol. 35, April, 2010.

Morozov et al., "Giant Intrinsic Carrier Mobilities in Graphene and Its Bilayer", Phys. Rev. Lett., vol. 100, p 16602, 2008

A. Akturk and N. Goldsman, "Electron transport and full-band electron-phonon interactions in graphene", J. Appl. Phys., vol. 103, p 053702, 2008.

J. S. Moon et al.,"Development toward wafer-scale graphene electronics", First International Symposium on Graphene and Emerging Materials for Post-CMOS Applications in 215th Electrochemical Society meeting, 2009.

C. Berger et al., J. Phys. Chem. B 108, 19912 (2004).

P. W. Sutter, J.-I. Flege, E. A. Sutter, "Epitaxial graphene on ruthenium". Nat. Mater. 7, 406–411, 2008.

C. Berger et al., "Electronic confinement and coherence in patterned epitaxial graphene," Science, vol. 312, pp. 1191–1196, 2006.

J. S. Moon et al., "Epitaxial Graphene RF Field-Effect Transistors on Si-face 6H-SiC Substrates", IEEE Electron Dev. Lett., vol. 60, pp 650-652, 2009.

Y. Q. Wu et al., "Top-gated graphene field-effect transistors formed by decomposition of SiC", Appl. Phys. Lett., vol. 92, p 092102, 2008.

J. Kedzierski et al., "Epitaxial Graphene Transistors on SiC Substrates", IEEE Trans. Electron Devices, vol. 55, pp 2078-2085, 2008.

J. S. Moon et al., " Top-gated Epitaxial Graphene FETs on Si-face SiC Wafers with a Peak transconductance of 600 mS/mm", IEEE Electron Dev. Lett., vol. 31, pp 260-262, 2010.

D. K. Gaskill et al., "Epitaxial Graphene Growth on SiC Wafers", ECS Transactions 19, p.117, 2009.

S. Takagi et al., "On the Universality of Inversion Layer Mobility in Si MOSFET's: Part I – Effects of Substrate Impurity Concentration", IEEE Trans. Electron Devices, vol. 41, pp 2357-2362, 1994.

Z.-Y. Cheng et al., "Electron Mobility Enhancement in Strained-Si n-MOSFETs Fabricated on SiGe-on-Insulator (SGOI) Substrates", IEEE Electron Dev. Lett., vol. 22, pp 321-323, 2001.

J. Hackley etal., "Graphitic carbon growth on Si(111) using solid source molecular beam epitaxy", Appl. Phys. Lett., vol. 95, p 133114, 2009.

M. Suemitsu et al., "Graphene formation on a 3C-SiC(111) thin film grown on Si(110) substrate", e-J Surf. Sci. Nanotech. vol. 7, pp. 311-313, 2009.

H-C Kang et al., "Epitaxial graphene top-gate FETs on silicon substrates", International Semiconductor Device Research Symposium, pp 1-2, 2009.

M. Fanton et al., "3C-SiC films grown on Si(111) substrates as a template for graphene epitaxy", First International Symposium on Graphene and Emerging Materials for Post-CMOS Applications in 215th Electrochemical Society meeting, 2009.
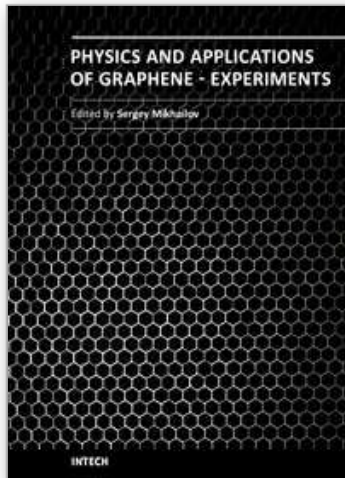
Physics and Applications of Graphene - Experiments

Edited by Dr. Sergey Mikhailov

The Stone Age, the Bronze Age, the Iron Age... Every global epoch in the history of the mankind is characterized by materials used in it. In 2004 a new era in material science was opened: the era of graphene or, more generally, of two-dimensional materials. Graphene is the strongest and the most stretchable known material, it has the record thermal conductivity and the very high mobility of charge carriers. It demonstrates many interesting fundamental physical effects and promises a lot of applications, among which are conductive ink, terahertz transistors, ultrafast photodetectors and bendable touch screens. In 2010 Andre Geim and Konstantin Novoselov were awarded the Nobel Prize in Physics "for groundbreaking experiments regarding the two-dimensional material graphene". The two volumes Physics and Applications of Graphene - Experiments and Physics and Applications of Graphene - Theory contain a collection of research articles reporting on different aspects of experimental and theoretical studies of this new material.

How to reference

In order to correctly reference this scholarly work, feel free to copy and paste the following:

Jeong-Sun Moon, Kurt Gaskill and Paul Campbell (2011). Graphene Transistors and RF Applications, Physics and Applications of Graphene - Experiments, Dr. Sergey Mikhailov (Ed.), ISBN: 978-953-307-217-3, InTech, Available from: http://www.intechopen.com/books/physics-and-applications-of-graphene-experiments/graphene-transistors-and-rf-applications

INTECH
open science | open minds